JOURNAL OF AIRCRAFT
Vol. 32, No. 4, July–August 1995

Estimating Noise Characteristics from Flight Test Data Using Optimal Fourier Smoothing

Eugene A. Morelli*
Lockheed Engineering and Sciences Company, Inc., Hampton, Virginia 23681-0001

A technique based on Fourier series analysis was developed to separate signal from noise for flight test data. This was done with an optimal filter designed in the frequency domain. The method is general, and separates signal and noise based on the spectral content of the measurement time history. Smoothed time histories with no time lag were computed, and noise characteristics were accurately estimated. The technique can be used independently of other procedures, and does not require assumptions about the independence of the noise processes or the frequency content of the measurements. Simulated data was used to demonstrate the technique and to evaluate the accuracy of estimated noise characteristics. For 20 simulation cases, noise standard errors were estimated within 5% of the true values. Flight test data from a lateral maneuver of the F-18 High Alpha Research Vehicle was then analyzed. The theoretical analysis was shown to be sound for both simulated data and flight test data.

Nomenclature

$A(i)$ = ith approximate area
a_y = lateral acceleration, g
b_k = kth Fourier sine series coefficient
C_n = noise model parameter
C_s = signal model parameter
f = frequency, Hz
f_k = frequency of the kth Fourier sine series term, Hz
f_N = Nyquist frequency, Hz
$g(i)$ = ith output with endpoint discontinuities removed
$\bar{g}(i)$ = Fourier sine series approximation for $g(i)$
$\bar{g}_s(i)$ = smoothed $\bar{g}(i)$
$\boldsymbol{g}$ = vector of $g(i)$ values
k = Fourier sine series frequency index
k_s = frequency index for the $|b_k|$ peak satisfying the signal tail criterion
N = total number of sample times
$N(f)$ = Fourier transform of the noise
$\bar{n}$ = noise mean value estimate
n_{avg} = number of $|b_k|$ peaks used to compute the noise model
$n(i)$ = noise for time $(i-1)\Delta t$
np = number of $|b_k|$ peaks
nz = number of measured outputs
p = body axis roll rate, rad/s
$\boldsymbol{R}$ = discrete noise covariance matrix
r = body axis yaw rate, rad/s
s_n^2 = noise variance estimate
T = data record length, s
T_k = period of the kth Fourier sine function
$Y(f)$ = Fourier transform of the signal
$\boldsymbol{Y}$ = $N \times nz$ matrix of smoothed output vectors
$y(i)$ = smoothed output for time $(i-1)\Delta t$
$Z(f)$ = Fourier transform of the measured time history
$\boldsymbol{Z}$ = $N \times nz$ matrix of measured output vectors
$z(i)$ = measured output for time $(i-1)\Delta t$
β = sideslip angle, rad
β_s = smoothed sideslip angle, rad
Δt = sampling interval, s
$\Phi(k)$ = optimal filter for the kth Fourier sine series term
ϕ = roll angle, rad

Superscripts
T = transpose
$\hat{}$ = estimate

Introduction

MATHEMATICAL modeling of aircraft dynamics based on flight test data involves experiment design, data compatibility analysis, model structure determination, parameter estimation, and model validation. In each of these tasks, it is useful to have some estimate of the measurement noise level, usually in the form of a noise covariance matrix.

Methods used to obtain this information include heuristic estimation based on instrument calibration or measured time history plots and estimating measurement noise covariance matrix elements as additional parameters along with aerodynamic and/or systematic instrumentation error parameters. The latter technique is used in conjunction with maximum likelihood estimation,[1] extended Kalman filter methods,[2] and filter-smoother algorithms.[3] Typically, the noise covariance matrix is assumed to be diagonal, with each noise variance on the diagonal considered an unknown parameter to be estimated. A consequence of this approach is that the overall order of the estimation problem is increased. A higher number of unknown parameters generally increases the computational burden, and can also adversely impact convergence because of identifiability problems.

Noise characteristics can also be estimated by smoothing measured time histories. Various schemes for local smoothing exist,[4] where the smoothed value at each data point is computed by fitting an assumed model to the point and its immediate neighbors, using least squares. The least squares operation filters the noise. This approach generally works well only for data with very low noise levels.

Application of digital filtering to measured time histories introduces time lag, so that all time histories of interest must be filtered identically to avoid time shifting the data improperly. The time lag problem can also be solved by filtering twice, forward and backward in time, for a net time lag of zero.[5] The cutoff frequency for digital filtering usually must be estimated from considerations such as the expected harmonic content of the signal based on experience. However, the cutoff frequency determined in this way will not be an

Presented as Paper 94-0152 at the AIAA 32nd Aerospace Sciences Meeting and Exhibit, Reno, NV, Jan. 10–13, 1994; received March 29, 1994; revision received Nov. 21, 1994; accepted for publication Nov. 22, 1994.

*Principal Research Engineer. Senior Member AIAA.

accurate frequency domain boundary between signal and noise for every measured time history. For example, the useful information in a typical airspeed measurement is confined to a smaller and lower frequency range compared to a typical pitch rate measurement, because of the inherent dynamics of aircraft. In addition, digital filters can introduce amplitude distortion in the passband.

The present work describes an alternative method for estimating the noise characteristics of measured time histories. The method uses Fourier series analysis and an optimal filter in the frequency domain to separate signal and noise. This result is then exploited in a simple scheme for estimating measurement noise covariance matrix elements.

The distinction between signal and noise has various interpretations. For example, output error techniques lump the modeling error together with the incoherent part of a measured time history and call this the measurement noise.[6] This viewpoint results in the measurement noise being colored and model-dependent. For the present work, measurement noise will be defined as the relatively broadband incoherent part of a measured time history. The term incoherent is meant to imply amplitude discontinuity and a lack of consistent phase-amplitude relationships, causing the autocorrelation function to be close to the impulse function. Heuristically, this part of the measured time history would be commonly recognized as having no deterministic component.

Measurement noise covariance estimates from the method proposed here would be useful when computing the information matrix for design and evaluation of parameter estimation experiments. In these situations, any noise covariance estimate that included some modeling error would be inappropriate. Data compatibility analysis typically involves difficulties related to parameter identifiability, so that an independent estimate of the noise covariance could help convergence and improve estimation accuracy. For modeling problems, accurate estimates of the measurement noise covariance as defined here would highlight model structure deficiencies by excluding modeling error from the noise estimates. For equation error methods, removing incoherent measurement noise in the regressors would more closely approximate noise-free regressors, which is assumed in the analysis.[7] In Kalman filter applications, the number of filter tuning parameters can be reduced when a good estimate of the measurement noise covariance matrix is available. Finally, the data smoothing process, which is a by-product of separating signal and noise, can be useful when analyzing very noisy measurements such as linear and angular accelerations.

The next section contains the theoretical development. Following this, an example using data from a nonlinear simulation is used to demonstrate the effectiveness of the method. Finally, the technique is applied to flight test data from the F-18 High Alpha Research Vehicle (HARV).

Theoretical Development

Problem Statement

Consider a time history $z(t)$, such as that shown in Fig. 1a. Assume a constant sampling rate, with a sample taken every Δt. The sampled version of $z(t)$ is then defined by

$$z(i) = z[(i-1)\Delta t] \qquad i = 1, 2, \ldots, N \tag{1}$$

The total time T is given by

$$T = (N-1)\Delta t \tag{2}$$

since $z(1)$ corresponds to time zero. The goal is to separate signal and noise, or equivalently to find $y(i)$ and $n(i)$ such that

$$z(i) = y(i) + n(i) \qquad i = 1, 2, \ldots, N \tag{3}$$

Assuming that the separation of noise and signal can be brought about, it is then useful to have some description of the noise characteristics. In many practical cases, the noise process can be assumed stationary and Gaussian, so that the noise characteristics can be described by the expected value and a constant variance. These quantities can be estimated from a finite data record using the relations

$$\bar{n} = \frac{1}{N}\sum_{i=1}^{N} n(i) \tag{4}$$

$$s_n^2 = \frac{1}{(N-1)}\sum_{i=1}^{N} [n(i) - \bar{n}]^2 \tag{5}$$

The strategy for determining the noise sequence $n(i)$ will be to find an accurate description in the frequency domain for the signal, then invert the Fourier transform to get $y(i)$, and use Eq. (3) in the form

$$n(i) = z(i) - y(i) \qquad i = 1, 2, \ldots, N \tag{6}$$

Solution Methodology

Fourier series expansion implicitly assumes that the time history under consideration is periodic. For the time history in Fig. 1a, as is generally true, making such an assumption implies discontinuities in the amplitude and first time derivative at the endpoints. Lanczos[4] shows that Fourier series for functions with these discontinuities have much slower convergence than the Fourier series for functions without discontinuities in the amplitude and the first derivative anywhere. In the former case, the magnitudes of the Fourier coefficients decrease asymptotically as k^{-1}, where k is the number of terms in the Fourier series expansion, whereas in the latter case the asymptotic decrease goes as k^{-3} (see Lanczos[4] for details). This seems reasonable since the sinusoids in the Fourier series have no discontinuities in amplitude or first derivative anywhere, and therefore, would be expected to have difficulty representing a time history with those characteristics. It is possible to remove the endpoint discontinuities for an arbitrary time history and thus achieve the more abrupt decrease in the magnitude of the Fourier coefficients, which corresponds to a faster convergence of the Fourier series expansion to the function. The importance of the higher rate of convergence will become clear in the subsequent discussion.

To remove the discontinuities, subtract a linear trend from the original time history in order to make the amplitudes at the endpoints equal to zero, then reflect the result about the origin. Define this new discrete time history as $g(i)$, with $g(-N) = g(1) = g(N) = 0$. The values of $g(i)$ are computed from

$$g(i) = z(i) - z(1) - (i-1)\left[\frac{z(N) - z(1)}{N-1}\right] \qquad i = 1, 2, \ldots, N \tag{7}$$

$$g(-i) = -g(i) \qquad i = 2, 3, \ldots, N \tag{8}$$

Figure 1b shows the result of performing these operations on the time history of Fig. 1a. The vector

$$\boldsymbol{g} = [g(-N), g(-N+1), \ldots, g(-2), g(1), g(2), \ldots, g(N)]^T \tag{9}$$

is an odd function of time, and thus may be expanded using a Fourier sine series

$$\tilde{g}(i) = \sum_{k=1}^{N-1} b_k \sin\left[\frac{k\pi(i-1)}{N-1}\right] \qquad i = 1, 2, \ldots, N \tag{10}$$

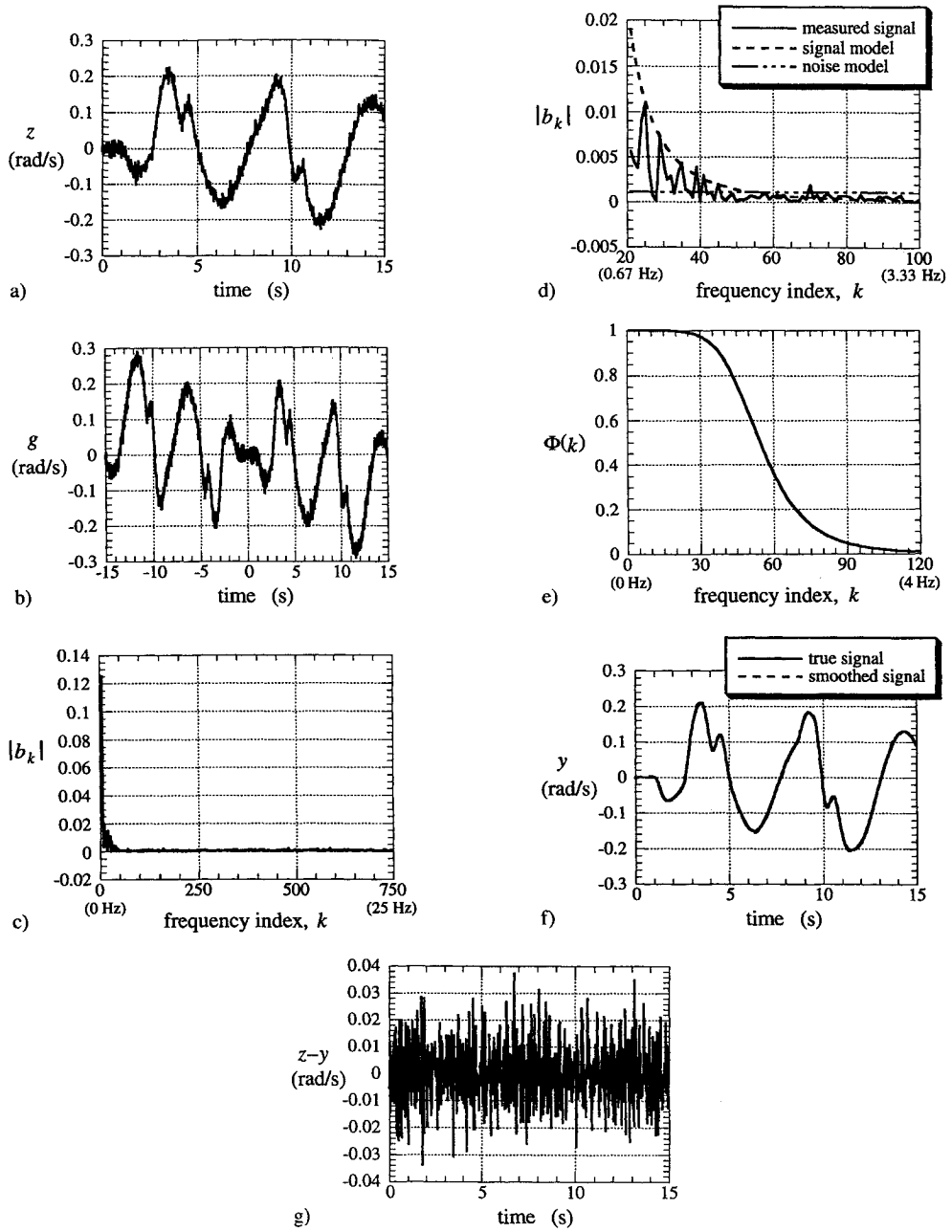

Fig. 1 a) Simulated roll rate, signal/noise ≈ 10.0; b) odd function with endpoint discontinuities removed corresponding to Fig. 1a; c) absolute Fourier sine series coefficients for simulated roll rate; d) expanded view of Fig. 1c, including signal and noise models; e) optimal filter for the simulated roll rate Fourier sine series coefficients; f) true and smoothed roll rate; and g) residuals computed using smoothed roll rate.

In Eq. (10), $\bar{g}(i)$ denotes the approximation to $g(i)$ using the Fourier sine series. The summation over frequency index k omits $k = 0$ (zero frequency), since this is a pure sine series. Only positive values of i are included in Eq. (10), because these values correspond to the original function. The abrupt k^{-3} decrease in the magnitudes of the Fourier sine series coefficients b_k can now be expected because the discontinuities in the amplitude and first time derivative at the endpoints have been removed. The Fourier sine series coefficients for g are given by[4]

$$b_k = \frac{2}{N-1}\sum_{i=2}^{N-1} g(i)\sin\left[\frac{k\pi(i-1)}{N-1}\right]$$
$$k = 1, 2, \ldots, N-1 \qquad (11)$$

where the index i runs from 2 to $N - 1$, because $g(1)$ and $g(N)$ are zero. The upper limit for k is $(N - 1)$, which corresponds to the Nyquist frequency.[8] From Eq. (10), the period of the kth Fourier sine series term T_k is given by

$$T_k = \frac{2(N-1)\Delta t}{k} \qquad (12)$$

and, therefore, the kth frequency f_k is related to the index k by

$$f_k = \frac{k}{2(N-1)\Delta t} \qquad (13)$$

In order to effectively smooth the data, it is necessary that the Nyquist frequency (equal to one-half the sampling rate for the data) be much higher than the highest frequency in the signal. This consideration is rarely a problem with modern data acquisition technology when proper attention is paid

to analog antialiasing filtering before sampling.[8] Airplane dynamics applications typically employ a sampling rate of at least 50 Hz, and the frequencies of interest rarely exceed 5 Hz.

Using Eqs. (7) and (8) to construct $\boldsymbol{g}$ guarantees that the endpoint discontinuities that result from assuming $\boldsymbol{g}$ to be periodic are in the second time derivative of the original time history. Convergence of the Fourier sine series approximation would be further improved if endpoint discontinuities in higher derivatives were also removed. However, since the measured time histories are from a dynamical system where application of forces can produce discontinuities in second-order (and higher) time derivatives, any attempt to remove additional endpoint discontinuities runs the risk of inadvertently modifying the signal. Therefore, removing amplitude and first time derivative endpoint discontinuities is accepted as the best that can be done without corrupting the desired signal in the course of removing endpoint discontinuities.

The Fourier sine series expansion in Eq. (10) contains all spectral components that can be computed from the given finite time history, including both signal and noise. The Fourier series for a coherent signal is fundamentally different than the Fourier series for noise. As mentioned above, a coherent signal with discontinuities in the second time derivative at the endpoints has Fourier series coefficient amplitudes that decrease asymptotically to zero with increasing k, i.e., $|b_k|$ is proportional to k^{-3}. On the other hand, since noise is incoherent and theoretically has constant power over the frequency range up to the Nyquist frequency, its Fourier series coefficients do not decrease asymptotically to zero, but instead have a relatively small and constant magnitude over all frequencies. This reflects the fact that the Fourier series expansion for an incoherent time history is divergent, due mainly to the inconsistent phase–amplitude relationships. In the case of a Fourier sine series, the Fourier series coefficients of the noise appear as a relatively constant amplitude oscillation about zero, representing random phase change in the spectral components. The abrupt k^{-3} decrease in the magnitudes of the Fourier sine coefficients for the signal contrasts sharply with the relatively constant magnitude of the Fourier sine series coefficients for the noise. The use of Eqs. (7) and (8) to remove endpoint discontinuities prior to performing the Fourier transform was done specifically to enhance this contrast.

The ideas presented to this point in the Solution Methodology section were based on material in Lanczos,[4] to which the reader is referred for more information. The remainder of this section describes the method developed to accurately separate signal and noise and the use of this result in estimating noise characteristics.

First, the optimal filter must be defined. Consider the Fourier transform of the measured time history, which is comprised of signal plus noise

$$Z(f) = Y(f) + N(f) \tag{14}$$

The goal is to design a frequency domain filter which is optimal in the sense of minimizing the squared difference between the true signal $Y(f)$ and the estimated signal $\hat{Y}(f)$ over the entire frequency range, i.e., the integral

$$\int_0^{f_N} \{\hat{Y}(f) - Y(f)\}^2 \, df \tag{15}$$

is to be minimized. The estimated signal in the frequency domain will be obtained by multiplying a filter $\Phi(f)$ with $Z(f)$

$$\hat{Y}(f) = \Phi(f)Z(f) = \Phi(f)[Y(f) + N(f)] \tag{16}$$

Substituting for $\hat{Y}(f)$ from Eq. (16) and recognizing that $Y(f)N(f)$ integrated over all frequencies will be approximately zero due to the incoherence of the noise, Eq. (15) becomes

$$\int_0^{f_N} \{\Phi^2(f)[Y^2(f) + N^2(f)] - 2\Phi(f)Y^2(f) + Y^2(f)\} \, df \tag{17}$$

Taking the derivative of the integrand in Eq. (17) with respect to $\Phi(f)$, setting the result equal to zero and solving for $\Phi(f)$ gives

$$\Phi(f) = \frac{Y^2(f)}{Y^2(f) + N^2(f)} \qquad 0 \le f \le f_N \tag{18}$$

or, in terms of the discrete frequency index k

$$\Phi(k) = \frac{Y^2(k)}{Y^2(k) + N^2(k)} \qquad 0 \le k \le N - 1 \tag{19}$$

Equation (18) gives the form of the optimal filter in the frequency domain, also called the Wiener filter.[8] For the problem at hand, an optimal filter can be designed in the frequency domain by taking advantage of the known analytical model forms for the Fourier sine series coefficients of signal and noise, discussed previously. Once analytical models for $Y(k)$ and $N(k)$ are identified, Eq. (19) can be used to construct the optimal filter $\Phi(k)$. This optimal filter then multiplies the b_k from Eq. (11). The smoothed signal (with endpoint discontinuities still removed) was computed from

$$\tilde{g}_s(i) = \sum_{k=1}^{N-1} \Phi(k) b_k \sin\left[\frac{k\pi(i-1)}{N-1}\right] \qquad i = 1, 2, \ldots, N \tag{20}$$

From theoretical considerations discussed previously, $|Y(k)|$ will be proportional to k^{-3}, while $|N(k)|$ will be approximately a constant. Therefore, $\Phi(k)$ from Eq. (19) will be near unity at low frequencies, passing the Fourier sine series components for the signal completely, then transition smoothly to near zero at high frequencies, removing Fourier sine series components associated with the noise. The summation in Eq. (20) need not be carried out over all $(N - 1)$ terms, because $|\Phi(k)b_k|$ becomes small as k increases. For the work described here, the summation was stopped when $|\Phi(k)b_k| < 1.0 \times 10^{-4}$.

The model for the magnitude variation of the Fourier sine series coefficients for the signal was $C_s k^{-3}$, with C_s a constant parameter to be determined. The model for the magnitude of the Fourier sine series coefficients for the noise was a constant C_n, with value to be determined. Figure 1c is a plot of the absolute values of the Fourier sine series coefficients from Eq. (11) for the time history of Fig. 1b, as a function of the frequency index k. The sample time Δt was 0.02 s, so that $N = 751$ for the 15-s time history shown in Fig. 1a. The sharp drop in the $|b_k|$ amplitudes for the signal can be contrasted with the relatively constant amplitude $|b_k|$ at high frequencies representing the divergence of the Fourier series for the noise. The goal is to compute simple analytical models for these two regions, in order to compute the optimal filter in the frequency domain from Eq. (19).

Figure 1d is an enlarged view of the $|b_k|$ amplitudes in the range of frequencies corresponding to $20 \le k \le 100$. It is apparent from this plot that the $|b_k|$ amplitudes are not monotonic with k, but are jagged with the peak values generally following the k^{-3} model. This reflects the fact that the time history contains discrete frequencies to varying degrees, causing the spectrum to be discontinuous. Therefore, the peak values were picked out numerically and ordered from greatest to smallest $|b_k|$ amplitude as k increases, so that the result was a set of $|b_k|$ peak amplitudes that were monotonically

decreasing with increasing k. This is roughly equivalent to approximating the spectrum using only the peak values of $|b_k|$. Assume that np peak values occur at frequency indices $k_1, k_2, \ldots, k_{np}$, with amplitudes $|b_{k_1}|, |b_{k_2}|, \ldots, |b_{k_{np}}|$, so that

$$k_1 < k_2 < \cdots < k_{np} \quad \text{and} \quad |b_{k_1}| > |b_{k_2}| > \cdots > |b_{k_{np}}| \tag{21}$$

Selected pairs of k_i and $|b_{k_i}|$, $i \in \{1, 2, \ldots, np\}$, can be used to generate a least squares fit to the $C_s k^{-3}$ model. In theory, the $C_s k^{-3}$ model holds asymptotically as k becomes large. In addition, the model should be as accurate as possible near the frequency index where $|Y(k)|$ and $|N(k)|$ are roughly equal. For these reasons, peak values in the vicinity of the tail of the $C_s k^{-3}$ model were used in the least squares fit to the signal model.

The change in area under the $C_s k^{-3}$ curve decreases as k increases. This fact was used to locate the tail of the cubic curve. Using the values from expression (21), the approximate area under the curve defined by the peak values is given by

$$A(i) = \sum_{j=2}^{i} \frac{1}{2}(|b_{k_j}| + |b_{k_{j-1}}|)(k_j - k_{j-1}) \qquad i = 2, 3, \ldots, np \tag{22}$$

where a simple trapezoidal Riemann sum was used to approximate the area. It was assumed that the tail of the cubic curve was reached when the change in $A(i)$ was 10% or less for two consecutive i values. The peak index where this occurred, denoted by k_s, was the smallest peak index that satisfied

$$\frac{A(s) - A(s-1)}{A(s)} \leq 0.1 \quad \text{for} \quad s \quad \text{and} \quad (s-1) \tag{23}$$

Estimation of C_s for the $C_s k^{-3}$ model was based on four peak index values: k_{s-2}, k_{s-1}, k_s, and k_{s+1}. The least squares problem for estimating C_s was set up as follows:

$$\boldsymbol{x} = \left[\frac{1}{(k_{s-2})^3}, \frac{1}{(k_{s-1})^3}, \frac{1}{(k_s)^3}, \frac{1}{(k_{s+1})^3}\right]^T \tag{24}$$

$$\boldsymbol{w} \equiv [|b_{k_{s-2}}|, |b_{k_{s-1}}|, |b_{k_s}|, |b_{k_{s+1}}|]^T \tag{25}$$

The least squares solution for C_s was

$$C_s = \boldsymbol{x}^T\boldsymbol{w}/\boldsymbol{x}^T\boldsymbol{x} \tag{26}$$

The expanded view in Fig. 1d shows the identified $C_s k^{-3}$ model on the same plot with the $|b_k|$ amplitudes. The constant model for the Fourier sine series coefficient magnitudes associated with the noise is also shown. A description of the computations required for the noise model is given next.

An estimate of C_n can be obtained by again considering only peak values of the $|b_k|$, where peak values were used to approximate the discontinuous noise spectrum, as before when considering $|b_k|$ for the signal. The constant value of the $|b_k|$ for the noise was computed as a rms average value using n_{avg} peak values immediately following the last peak value used in the cubic function fit, so that

$$C_n = \left[\sum_{j=s+2}^{s+n_{\text{avg}}+1} \frac{(b_{k_j})^2}{n_{\text{avg}}}\right]^{1/2} \tag{27}$$

where a reasonable value for n_{avg} was found to be

$$n_{\text{avg}} = N/10 \tag{28}$$

with n_{avg} rounded off to the nearest integer and assuming a fairly large N, i.e., $N \geq 200$.

The constant C_n from Eq. (27) was the model for the $|b_k|$ associated with the noise, as shown in Fig. 1d. Then, for computing the optimal filter

$$Y(k) = C_s k^{-3} \tag{29}$$

$$N(k) = C_n \tag{30}$$

The design parameters used in Eqs. (23) and (27) were reasonable values chosen by trial and error to give the most accurate and robust analytical models for $Y(k)$ and $N(k)$. In practice, there is some room for error in this modeling because the $|b_k|$ values are small in this region anyway, and therefore, excluding or including a few components improperly in Eq. (20) will have minimal adverse effect on the final smoothed time history and the noise covariance estimate. Additional margin for error in the analytical modeling of Eqs. (29) and (30) is provided by the fact that the frequency domain filter computed from Eq. (19) is the optimal filter if the models in Eqs. (29) and (30) are exact.

Naturally, some components of the noise lie in the low frequency range, but there is no way to distinguish this noise from the signal, which also resides in the low-frequency range. Typically, the large majority of the noise power resides at high frequency relative to the frequencies of the signal, and this noise can be removed very effectively. When the signal-to-noise ratio is high, the power of the noise relative to that of the signal is small in an overall sense, but this situation is improved by the fact that the noise power is spread over a wide frequency range, whereas the signal power is limited to low frequencies. Once the high frequency noise has been removed, the remaining noise components in the frequency range of the signal have very low power, and therefore, have little impact on the smoothing operation and the noise covariance estimation.

As a final step, the linear trend removed from the original time history using Eq. (7) must be restored to the smoothed values $\bar{g}_s(i)$ from Eq. (20). The smoothed values $y(i)$ result from

$$y(i) = \bar{g}_s(i) + z(1) + (i-1)\left[\frac{z(N) - z(1)}{N-1}\right] \qquad i = 1, 2, \ldots, N \tag{31}$$

It is clear from Eqs. (7) and (31) that the endpoints of the original time history, $z(1)$ and $z(N)$, are completely excluded from all smoothing operations. For very noisy data, this can produce significant error in the smoothed time history. To correct for this, the endpoints only were smoothed by a low pass filter implemented as a time convolution with a fixed weighting function[9] prior to applying the Fourier smoothing technique described previously. The cutoff frequency for this filter was fixed at 5 Hz, which is relatively high for flight test data intended for studying airplane dynamics.

The noise sequence $n(i)$, $i = 1, 2, \ldots, N$, was obtained from Eq. (6) using the $y(i)$ computed from Eq. (31). Equations (4) and (5) were then used to estimate the noise characteristics. For an experiment with nz measured outputs, the measured time histories can be arranged in an $N \times nz$ matrix

$$\boldsymbol{Z} \equiv [z_1, z_2, \ldots, z_{nz}] \tag{32}$$

where z_i, $i = 1, 2, \ldots, nz$, are $N \times 1$ vectors of measured time histories. Similarly, define

$$\boldsymbol{Y} \equiv [y_1, y_2, \ldots, y_{nz}] \tag{33}$$

where y_i, $i = 1, 2, \ldots, nz$, are $N \times 1$ vectors of the respective smoothed signal time histories. An estimate of the measurement noise covariance matrix $\hat{R}$ was obtained from

$$\hat{R} = \frac{(Z - Y)^T(Z - Y)}{N - 1} \tag{34}$$

Results

Figure 1a depicts aircraft roll rate in rad/s from a nonlinear simulation. The added measurement noise was zero mean white Gaussian, with standard error set to one-tenth the rms of the uncorrupted signal, making the signal-to-noise ratio approximately 10 to 1. The standard error of the added noise was known and equal to 0.0112 rad/s. Figure 1d shows an expanded view of the signal and noise models, $Y(k)$ and $N(k)$, respectively, on the same plot with the $|b_k|$ from the measurement time history. The optimal filter computed from Eq. (19) appears in Fig. 1e. An effective cutoff frequency can be computed as the frequency where $Y(k) = N(k)$ or $\Phi(k) = 0.5$. For Fig. 1e, the cutoff frequency index was 54, corresponding to 1.8 Hz from Eq. (13) ($N = 751$, $\Delta t = 0.02$ s). In Fig. 1f, the smoothed signal and the true signal are seen to be virtually identical. Figure 1g shows that the residuals are very close to zero mean with no deterministic component.

To assess the accuracy of the noise estimates using Eqs. (4–6) and (31), 20 runs were made by corrupting the same true signal used for Fig. 1a with noise from 20 different realizations of a zero mean, white Gaussian noise process. Noise amplitude was selected to reduce the signal-to-noise ratio to approximately 5 to 1. The results are given in Table 1. The standard error of the noise was estimated within 5% of the true value for every case.

Next, data from a flight test maneuver of the F-18 HARV was analyzed. The sideslip angle measurement from a sensor located on the right wingtip boom is plotted in Fig. 2a. The 30-s time history was sampled at 50 Hz ($N = 1501$, $\Delta t = 0.02$). Figure 2b shows the Fourier sine series magnitudes with the cubic decrease in the $|b_k|$ at low frequency, but also including components of an apparent structural mode near 9 Hz. Figure 2b indicates that virtually all the deterministic signal power for rigid body motion lies below approximately 1 Hz. Note also in Fig. 2b that the $|b_k|$ for the deterministic signal associated with the structural mode also exhibits the asymptotic cubic decrement in magnitude with increasing frequency. Figure 2c is an expanded plot of the $|b_k|$ with corresponding signal and noise models. The $|b_k|$ variation for the signal and noise are represented well by the analytical models, demonstrating that the technique readily adapted to the measured time history spectrum. The optimal filter is shown in Fig. 2d as a function of frequency. Cutoff frequency was $k = 45$ or 0.75 Hz. Smoothed sideslip angle β_s is plotted in Fig. 2e. The residuals in Fig. 2f show approximately zero mean and some deterministic components resulting from the structural vibration.

Noise covariance matrix elements were estimated using Eq. (34) for five measured outputs from the same flight test maneuver. The results are given in Table 2. Graphical results for these measurements were similar to those shown in Fig. 2.

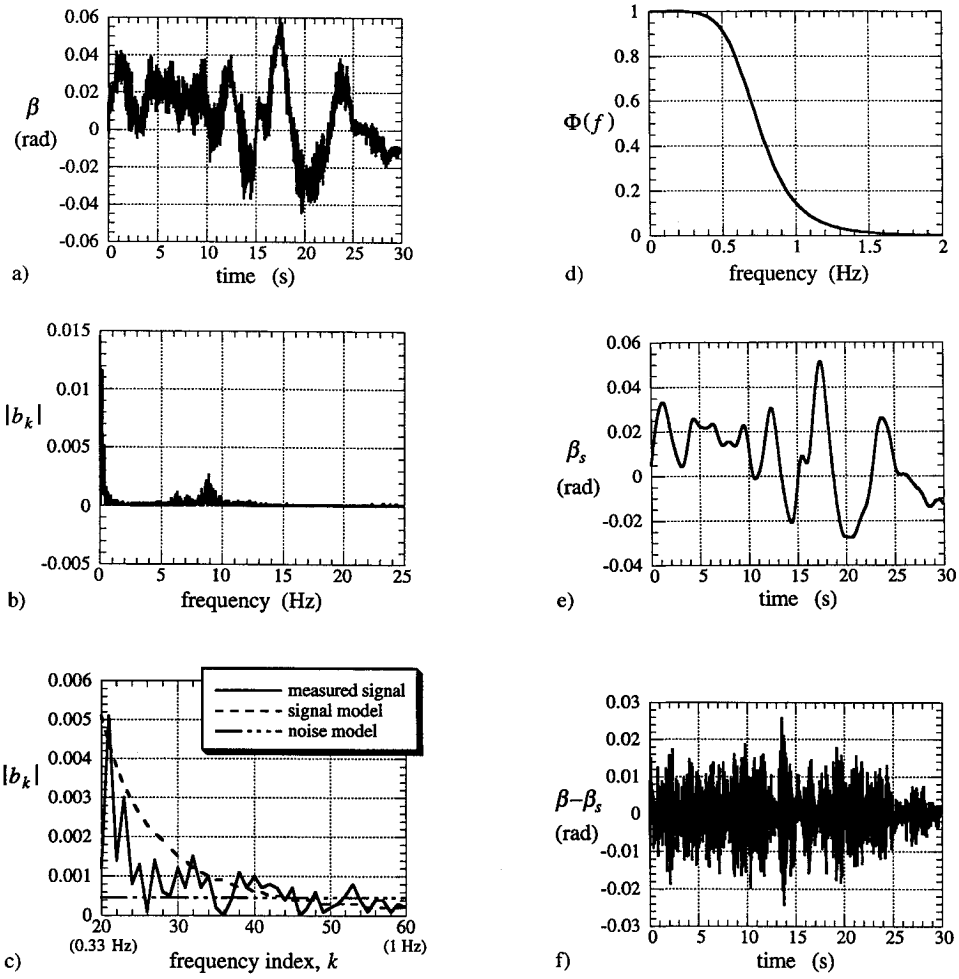

Fig. 2 a) Measured sideslip angle; b) absolute Fourier sine series coefficients for measured sideslip angle; c) expanded view of Fig. 2b, including signal and noise models; d) optimal filter for the measured sideslip angle Fourier sine series coefficients; e) smoothed sideslip angle; and f) residuals computed using smoothed sideslip angle.

Table 1 Noise standard error estimates from simulation data

Run number	Noise standard error estimate, s_n	True noise standard error	% error
1	0.0273	0.0282	−3.3
2	0.0274	0.0281	−2.4
3	0.0290	0.0296	−2.2
4	0.0290	0.0299	−3.0
5	0.0263	0.0273	−3.8
6	0.0262	0.0272	−3.4
7	0.0269	0.0280	−3.9
8	0.0274	0.0285	−4.1
9	0.0282	0.0291	−3.1
10	0.0285	0.0295	−3.5
11	0.0283	0.0281	0.9
12	0.0278	0.0291	−4.5
13	0.0280	0.0287	−2.1
14	0.0265	0.0278	−4.8
15	0.0266	0.0272	−2.1
16	0.0276	0.0286	−3.7
17	0.0275	0.0286	−3.9
18	0.0276	0.0286	−3.3
19	0.0269	0.0279	−3.7
20	0.0279	0.0287	−2.9

Table 2 Measurement noise covariance matrix estimated from flight test data ($\times 10^3$)

	β	p	r	ϕ	a_y
β	0.0484	0.0218	−0.0001	0.0022	−0.0037
p	—	0.1999	−0.0041	−0.0020	0.3381
r	—	—	0.0121	0.0005	0.0220
ϕ	—	—	—	0.0058	0.0288
a_y	—	—	—	—	3.2004

Concluding Remarks

Fourier series analysis was used to design an optimal filter in the frequency domain for accurately separating signal and noise. The optimal filter was designed using simple analytical models identified from both theoretical analysis and the spectrum of the measured time history. The method produced smoothed time histories with zero lag relative to the measured time histories, and gave an independent and accurate estimate of the noise characteristics. No assumptions about the independence of the noise sequences were required. Using simulated data, it was shown that noise characteristics could be very accurately estimated.

Analytical model fits in the frequency domain and time domain residuals for measured sideslip angle from the F-18 HARV indicated an accurate and effective separation of signal and noise for flight test data. A method for estimating the noise covariance matrix for multiple measured outputs was demonstrated using F-18 HARV flight test data. Such information can be used to replicate flight test measurement noise in simulations.

The smoothed time histories and estimates of the noise characteristics resulting from the technique described in this work can be useful in designing and evaluating experiments, and in various techniques for data compatibility analysis, model structure determination, parameter estimation, and model validation.

Acknowledgments

This research was conducted at the NASA Langley Research Center under NASA Contract NAS1-19000. Discussions with Vladislav Klein of the George Washington University contributed to the work presented here.

References

[1]Klein, V., and Morgan, D. R., "Estimation of Bias Errors in Measured Airplane Responses Using Maximum Likelihood Method," NASA TM 89059, Jan. 1987.

[2]Klein, V., and Schiess, J. R., "Compatibility Check of Measured Aircraft Responses Using Kinematic Equations and Extended Kalman Filter," NASA TN D-8514, Aug. 1977.

[3]Bach, R. E., Jr., "State Estimation Applications in Aircraft Flight Data Analysis," NASA RP 1252, March 1991.

[4]Lanczos, C., *Applied Analysis*, Dover, New York, 1988, Chaps. 4 and 5.

[5]Simon, W. E., "Digital Low-Pass Filter Without Phase Shift," NASA Tech Brief KSC-11471, July 1993.

[6]Maine, R. E., and Iliff, K. W., "The Theory and Practice of Estimating the Accuracy of Dynamic Flight-Determined Coefficients," NASA RP 1077, July 1981.

[7]Klein, V., "Estimation of Aircraft Aerodynamic Parameters from Flight Data," *Progress in Aerospace Sciences*, Vol. 26, Pergamon, Oxford, England, UK, 1989, pp. 1–77.

[8]Press, W. H., Flannery, B. P., Teukolsky, S. A., and Vetterling, W. T., *Numerical Recipes (FORTRAN Version)*, Cambridge Univ. Press, New York, 1989, Chap. 12.

[9]Graham, R. J., "Determination and Analysis of Numerical Smoothing Weights," NASA TR R-179, Dec. 1963.